# Ocean acidification alters morphology of all otolith types in Clark's anemonefish (*Amphiprion clarkii*)

Robert J. Holmberg 1, Eric Wilcox-Freeburg, Andrew L. Rhyne<sup>2,3</sup>, Michael F. Tlusty, Alan Stebbins, Steven W. Nye Jr., Aaron Honig, Amy E. Johnston, Christine M. San Antonio, Bradford Bourque, Robyn E. Hannigan

Published January 7, 2019 PubMed 30643693

Ocean acidification, the ongoing decline of surface ocean pH and  $[CO_3^{2-}]$  due to absorption of surplus atmospheric CO<sub>2</sub>, has far-reaching consequences for marine biota, especially calcifiers. Among these are teleost fishes, which internally calcify otoliths, critical elements of the inner ear and vestibular system. There is evidence in the literature that ocean acidification increases otolith size and alters shape, perhaps impacting otic mechanics and thus sensory perception. Here, larval Clark's anemonefish, Amphiprion clarkii (Bennett, 1830), were reared in various seawater pCO<sub>2</sub>/pH treatments analogous to future ocean scenarios. At the onset of metamorphosis, all otoliths were removed from each individual fish and analyzed for treatment effects on morphometrics including area, perimeter, and circularity; scanning electron microscopy was used to screen for evidence of treatment effects on lateral development, surface roughness, and vaterite replacement. The results corroborate those of other experiments with other taxa that observed otolith growth with elevated pCO<sub>2</sub>, and provide evidence that lateral development and surface roughness increased as well. Both sagittae exhibited increasing area, perimeter, lateral development, and roughness; left lapilli exhibited increasing area and perimeter while right lapilli exhibited increasing lateral development and roughness; and left asterisci exhibited increasing perimeter, roughness, and ellipticity with increasing pCO<sub>2</sub>. Right lapilli and left asterisci were only impacted by the most extreme pCO<sub>2</sub> treatment, suggesting they are resilient to any conditions short of aragonite undersaturation, while all other impacted otoliths responded to lower concentrations. Finally, fish settlement competency at 10 dph was dramatically reduced, and fish standard length marginally reduced with increasing pCO2. Increasing abnormality and asymmetry of otoliths may impact inner ear function by altering otolithmaculae interactions.

"Core development" in the rubric has been renamed "lateral development" in the manuscript. In the rubric, "core" refers not to the otolith's core but to the center of its lateral face.

# Introduction

Since the advent of the industrial revolution, humankind has inadvertently relocated a significant volume of carbon to the troposphere, where it now resides as a greenhouse gas, warming the earth via radiative forcing (IPCC, 2013). Global warming, however, is not the sole consequence of surplus atmospheric CO<sub>2</sub>: the surface ocean has absorbed approximately 30% of anthropogenic CO<sub>2</sub> emissions (Mikaloff Fletcher et al., 2006; Le Quéré et al., 2010), contributing to ocean acidification (Caldeira & Wickett, 2003). While this absorption is an important sink, abating the greenhouse effect (IPCC, 2013), it has consequences for marine ecosystems. Following diffusion, aqueous CO<sub>2</sub> impacts seawater chemistry by reducing pH and carbonate ( $CO_3^{2-}$ ) concentration (Doney et al., 2009). Both will impact the fitness of marine biota, with cascading effects up to the ecosystem level (Fabry et al., 2008; Queirós et al., 2015; Hoegh-Guldberg et al., 2017). From population abundances to community shifts, ocean acidification has the potential to alter the ecological landscape of the ocean (Gaylord et al., 2015).

The declining availability of free  $CO_3^{2-}$  is particularly worrisome due to its implications for marine calcifiers, which use calcium carbonate (CaCO<sub>3</sub>) to form body structures including shells, teeth, and spines. Surface waters are normally supersaturated with  $CO_3^{2-}$ , but as  $[CO_3^{2-}]$  decreases, calcifiers may struggle to precipitate  $CaCO_3$  (Gattuso & Buddemeier, 2000). Furthermore, if seawater is undersaturated with respect to calcium carbonate minerals (e.g., aragonite,  $\Omega_{Ar}$ ), existing structures may readily dissolve (Orr et al., 2005). A vast body of literature expounds ocean acidification's anticipated effects on calcifier fitness in the future ocean,

demonstrating variable degrees of severity (Hendriks, Duarte & Álvarez, 2010; Kroeker et al., 2013). Differential responses may depend on the specific biochemical pathways involved in calcification (Ries, Cohen & McCorkle, 2009), biological mechanisms for buffering pH changes in body fluids (Munday et al., 2011a), energetics limiting physiological acclimation (Seibel, Maas & Dierssen, 2012), or various ecological forces acting on an organism (Kroeker, Micheli & Gambi, 2012).

Teleostei is an extremely diverse infraclass of Actinopterygii representing the modern bony fishes, comprised of more than 30,000 species and dominating most aquatic habitats (Froese & Pauly, 2018). Teleosts are internal calcifiers, precipitating CaCO<sub>3</sub> in the intestinal lumen that aids water absorption and osmoregulation (Grosell, 2011), and precipitating otoliths in the inner ear that are critical for mechanoreception (Moyle & Cech, 2004). Heuer & Grosell (2014) reviewed numerous effects of acidification on marine teleosts, including respiratory acidosis leading to sustained elevation of blood plasma HCO<sub>3</sub> (Esbaugh, Heuer & Grosell, 2012), cognitive disruption and behavioral changes linked to inhibited GABA<sub>A</sub> neurotransmitter receptor function (Nilsson et al., 2012), mixed impacts on standard and maximum metabolic rates with implications for aerobic scope (Munday, Crawley & Nilsson, 2009), and increased otolith area (Munday et al., 2011b) and mass (Bignami, Sponaugle & Cowen, 2013; Bignami et al., 2013). As such, otoliths may be points of vulnerability for teleosts in the near-future ocean (Ishimatsu, Hayashi & Kikkawa, 2008; Munday et al., 2008; Heuer & Grosell, 2014).

Otoliths, or ear stones, are critical features located within the inner ear of teleost fishes, formed by precipitation of CaCO<sub>3</sub> around a protein-rich matrix and bathed in endolymph (Panella, 1971). CaCO<sub>3</sub> supersaturation is maintained in the endolymph by proton pumps in the epithelial cells adjacent to the site of crystallization, which maintain the pH gradient required for CO<sub>3</sub><sup>2-</sup> - HCO<sub>3</sub><sup>-</sup> balance (Ishimatsu, Hayashi & Kikkawa, 2008). Otoliths exist in three pairs (sagittae, lapilli, asterisci), with one from each pair contained within each otolithic end organ. When disturbed by fish movement or sound waves, otoliths trigger sensory maculae lining the interior wall of their chambers, converting the force into electrical impulses interpreted by the brain. Likewise, otoliths function as sensory organs for hearing and gravisense (Popper & Fay, 1993).

Researchers recognize the potential for ocean acidification to impact otolith growth in teleosts, especially during the sensitive larval phase, and many have demonstrated effects experimentally (Table 1). Contrary to the hypothesis that ocean acidification will inhibit otolith growth due to dwindling CO<sub>3</sub><sup>2-</sup> availability (Ishimatsu, Hayashi & Kikkawa, 2008), elevated seawater pCO<sub>2</sub> stimulates growth of sagittae and/or lapilli in many taxa. This growth is attributed to elevated blood plasma [HCO<sub>3</sub><sup>-</sup>], retained to buffer acidosis and transported into the endolymph where it becomes substrate for CO<sub>3</sub><sup>2-</sup> aggregation (Checkley et al., 2009; Munday et al., 2011b; Heuer & Grosell, 2014). Only one study (Mu et al., 2015) observed decreased otolith size in response to elevated pCO<sub>2</sub>. Other studies (Franke & Clemmesen, 2011; Munday et al., 2011a; Simpson et al., 2011; Frommel et al., 2013; Perry et al., 2015; Cattano et al., 2017; Martino et al., 2017; Jarrold & Munday, 2018) observed no effects of pCO<sub>2</sub> on otolith morphology.

Table 1:

Summary of observed ocean acidification impacts on otolith morphology. In the 'Metrics' column, S denotes effects of  $pCO_2$  on sagittae and L denotes effects on lapilli. Metrics that increased at elevated  $pCO_2$  are designated with an up arrow; metrics that decreased at elevated  $pCO_2$  are designated with a down arrow. The 'Min. Effect' column represents the minimum  $pCO_2$  threshold for which any effect was observed, reported to the decimal place published.

Citation	Species	Life Stage	Metrics	Min. Effect (µatm)
Checkley et al. (2009)	Atractoscion nobilis	Larval	↑ S Area	993
Munday et al. (2011b)	Amphiprion percula	Larval	↑ S Area, Length	1,721.4
Hurst et al. (2012)	Theragra chalcogramma	Juvenile	↑ S Mean Incr. Width	478
Bignami, Sponaugle & Cowen (2013), Bignami et al. (2013)	Rachycentron canadum	Larval	↑ S Mass; ↑ S,L Area, Vol., Dens., ↓ Area/Vol.	800
Maneja et al. (2013)	Gadus morhua	Larval	↑ S,L Area; ↑ S Roundness; ↓ L Roundness	1,800
Bignami, Sponaugle & Cowen (2014)	Coryphaena hippurus	Larval	↑ S,L Area	1,190
Pimentel et al. (2014)	Solea senegalensis	Larval	↑ S Area	1,600
Schade, Clemmesen & Wegner (2014)	Gasterosteus aculeatus	Juvenile	↑ S Area	1,167
Mu et al. (2015)	Oryzias melastigma	Larval	↓ S Area	2,372.6
Réveillac et al. (2015)	Sparus aurata	Juvenile	↑ S Calc. Rate, Area/TL, ↓ Roundness	726
Shen et al. (2016)	Atractoscion nobilis	Larval	↑ S,L Area	2,500
Faria et al. (2017)	Argyrosomus regius	Larval	↑ S Area, Perimeter, Width	1,900
	Diplodus sargus	Larval	↑ S Area, Perimeter	1,100
	Solea senegalensis	Larval	↑ S Area, Perimeter	1,900
Martins (2017)	Lepadogaster lepadogaster	Larval	↑ S Roundness	1,541.68
Mirasole et al. (2017)	Diplodus vulgaris	Juvenilea	↑ S Relative Length; Altered Shape	pH 7.8 <sup>b</sup>
	Gobius bucchichi	Adult <sup>a</sup>	S Altered Shape	pH 7.8 <sup>b</sup>
Coll-Lladó et al. (2018)	Sparus aurata	Larval	↑ S,L Area, Perimeter, Shape Irregularity	1,159

DOI: 10.7717/peerj.6152/table-1

### Notes:

<sup>a</sup>Life stage, although unlisted in the manuscript, is here inferred from fish standard length (SL).

<sup>b</sup>pCO<sub>2</sub> is unlisted in the manuscript and cannot be calculated without additional seawater carbonate chemistry parameter(s).

Evidence that acidification alters otolith size and shape has inspired hypotheses that this could interfere with otic mechanics, and thus impair sensory perception in teleosts (e.g., Munday et al., 2011b; Bignami et al., 2013; Bignami, Sponaugle & Cowen, 2014). Indeed, there is some evidence that asymmetry of otolith size, shape, and mass may impair auditory/vestibular function in some species with consequences for habitat detection and overall fitness (Lychakov & Rebane, 2005; Gagliano et al., 2008; Anken, Knie & Hilbig, 2017). Others have added that increased otolith size from ocean acidification could enhance auditory sensitivity to the benefit or detriment of the fish depending on life history (Bignami et al., 2013; Bignami, Sponaugle & Cowen, 2014; Réveillac et al., 2015).

While most available studies quantified simple morphometrics to analyze pCO<sub>2</sub> effects on otolith morphology, the most informative among them augmented morphometrics with other analyses, including complex shape analyses (e.g., Fourier analysis) (Munday et al., 2011a;

Munday et al., 2011b; Simpson et al., 2011; Martino et al., 2017; Mirasole et al., 2017); mass, volume and density analyses (Bignami, Sponaugle & Cowen, 2013; Bignami et al., 2013); and compositional analyses (e.g., LA-ICPMS) (Munday et al., 2011b; Hurst et al., 2012; Martino et al., 2017; Mirasole et al., 2017; Coll-Lladó et al., 2018). Similarly, scanning electron microscopy can be used to screen for treatment effects on aspects of otolith morphology and composition that, although typically overlooked in simple morphometric analysis, may impact ear function. These may include: (i) lateral development, defined as the degree of convexity of an otolith's lateral face; (ii) percent visible crystals, defined as an estimate of surface crystal density or grain, approximating surface roughness; (iii) crystal habit, here defined as any deviation in crystal shape from the predominant orthorhombic aragonite in sagittae and lapilli, or hexagonal vaterite in asterisci; and (iv) overall mineralogy, here defined as relative proportion of orthorhombic aragonite versus hexagonal vaterite visible on an otolith's surface. The former two metrics estimate an otolith's surface topography and texture, and the latter two estimate crystal features indicative of composition, density, and stability under environmental stress (Boulos et al., 2015). These metrics are intended as first-pass screening tools for efficiently identifying general trends in the data; should they yield compelling evidence of treatment differences, they could be followed with more rigorous methods to best quantify the variable (e.g., measuring otolith height directly or determining CaCO<sub>3</sub> polymorph composition with Raman spectroscopy (Coll-Lladó et al., 2018)).

In addition to standard morphometrics, the mineralogical metrics described above were used to investigate ocean acidification impacts on otolith morphology in larval Clark's anemonefish, *Amphiprion clarkii* (Bennett, 1830). *A. clarkii* is a teleost reef fish belonging to Pomacentridae and inhabiting shallow reefs throughout the Indo-Pacific (Froese & Pauly, 2018). The species was chosen both as a novel taxon and to enable intragenus comparison with previous work (Munday et al., 2011b). Any impacts on its otolith morphology could have implications for teleost sensory perception and fitness in the future ocean.

# **Materials & Methods**

### Livestock

All husbandry was completed at Roger Williams University in Bristol, Rhode Island, USA (IACUC #R-11-09-13). Several *Amphiprion clarkii* (Bennett, 1830) broodstock pairs were reared, all wild-caught in Fiji and acquired from Long Island Aquarium, Riverhead, New York, USA. Broodstock periodically laid clutches of eggs on porcelain tiles in aquaria (every 10–12 days). One large, healthy clutch was selected from a single broodstock pair, removed the night before anticipated day of hatch (around day eight post-deposition), and placed in a separate, aerated, 200 L hatching aquarium. Upon hatch, *A. clarkii* larvae were randomly distributed into 40 L experimental aquaria at a density of 40 individuals per aquarium. Throughout the experimental trial, larvae were fed ad libitum with wild copepods from monoculture (*Pseudodiaptomus spp.*) in a background of algae (*Isochrysis spp.*). *Pseudodiaptomus spp.* were dosed to densities of 5 mL<sup>-1</sup> and 1 mL<sup>-1</sup> (nauplii and adults respectively), as measured using a counting wheel, and *Isochrysis spp.* twice daily to maintain a concentration of 40,000 cells mL<sup>-1</sup>, as measured using a cell counter (Beckman Coulter Inc., Brea, CA).

### **Experimental trial**

The experimental design consisted of four pCO<sub>2</sub>/pH treatments selected to model various present and anticipated future ocean conditions: (i) 350 µatm/pH 8.16 (control), modern ocean conditions; (ii) 800 μatm/pH 7.80, approximate conditions projected for 2100 under Representative Concentration Pathway (RCP) 8.5 (IPCC, 2013); (iii) 1,600 µatm/pH 7.60, nearly double 2,100 levels under RCP 8.5 (IPCC, 2013); (iv) 3,000 μatm/pH 7.30, a reasonable extreme given coastal eutrophication-induced acidification (Wallace et al., 2014), and given that eutrophication is already occurring in some reef systems inhabited by A. clarkii (Bell, Elmetri & Lapointe, 2014; Fabricius, 2005). Treatments were replicated three times and assigned to 12 experimental units (aquaria) in a randomized design. Seawater was sourced from Mt. Hope Bay, sterilized using sodium hypochlorite and UV light, filtered to 1 µm, and used to fill experimental aquaria. 25% water changes were completed every other day using drip buckets at 100 mL min<sup>-1</sup>. Seawater salinity and temperature were measured twice daily in all aquaria using a handheld meter (YSI, Yellow Springs, OH). Seawater total alkalinity was measured once every other day in all aquaria using a tabletop autotitrator (Hanna Instruments, Smithfield, RI). The experimental trial took place within an environmental chamber to maintain ambient air conditions at 28 °C, and aquaria were covered with loose fitting lids to minimize CO2 outgassing and evaporative heat loss. Seawater was aerated with house-supplied air connected to airstones to maintain dissolved oxygen. Experimental treatments were achieved and maintained by dosing CO<sub>2</sub> gas through the airstones using a CO<sub>2</sub> dosing apparatus (Wilcox-Freeburg et al., 2013) controlled by hobbyist aquarium controllers (Digital Aquatics, Woodinville, WA). pH<sub>T</sub> of each aquarium was measured continuously using research-grade glass combination electrodes calibrated to synthetic seawater

buffers (Byrne, 1987; Millero et al., 1993), prepared from analytical reagent grade chemicals (Fisher Scientific, Hampton, NH). The aquarium controller output pH<sub>T</sub> data every 1-3 s via RSS feed, which was parsed/logged to a PC with custom Perl and MATLAB scripts (Wilcox-Freeburg, 2014) (Perl Version 5.28.0, https://www.perl.org/; MATLAB Version R2017b, https://www.mathworks.com/products/matlab.html). Average DIC, pCO<sub>2</sub>, and  $\Omega_{Ar}$  were calculated for each aquarium from measured seawater parameters using CO2calc (https://soundwaves.usgs.gov/2011/03/research4.html). The experimental trial concluded after 10 days, at the onset of fish metamorphosis.

### **Data collection**

Upon conclusion of the experimental trial, and following euthanization of fish with a lethal dose of tricaine mesylate (MS-222) in seawater, each individual was counted, placed on a Sedgewick rafter (1 mm), and photographed with a digital camera-equipped stereomicroscope at 10×-90× magnification. Mortality counts (by aquarium) were calculated by subtracting final fish counts from initial stocking density. Standard lengths of each individual were measured to 1/100 mm from stereomicrographs with ImageJ (Version 1.51n; https://imagej.nih.gov/ij/), and averaged by aquarium (arithmetic mean). Settlement competency was determined according to behavioral and morphological criteria; larvae were considered competent to settle when they began to cling to an aquarium wall rather than swim freely in the water column, and concurrently develop pigmentation consistent with settlement-stage metamorphosis. Due to natural variance in ontogeny among individuals, some had not achieved settlement competency when the experimental trial ended at 10 days post hatch (dph). Proportions of surviving fish that achieved settlement competency by 10 dph versus those that had not were tallied for each aquarium. Nonsettlement-stage fish data (standard length, otolith morphometric variables, otolith mineralogical variables) were excluded from all further analyses (sample exclusion criteria were preestablished: 38 fish, or roughly 15% of surviving fish, were excluded). Next, all six otoliths (two each of sagittae, lapilli, and asterisci) were manually removed under a polarizing stereo dissecting microscope. Each set of otoliths was digitally photographed with the stereomicroscope at 90x magnification and mounted to aluminum scanning electron microscopy (SEM) stubs for later analysis. Area, perimeter, major axis, and minor axis of all six otoliths from all fish were quantified from stereomicrographs with custom MATLAB image analysis software (Wilcox-Freeburg, 2014) (MATLAB Version R2017b; https://www.mathworks.com/products/matlab.html). All otolith morphometrics were measured to 1/100 unit. Otolith circularity was calculated from major and minor axes  $(\frac{\pi \times (\text{minor axis}/2)^2}{\pi \times (\text{major axis}/2)^2})$ . Aquarium means for each morphometric variable were determined by calculating the arithmetic mean of data from all individual fish within each aquarium (grouped by otolith type and side). Due to moderate-strong correlations between standard length and otolith area and perimeter at the evaluation unit (individual fish) level (area: r > 0.49, perimeter: r > 0.30 for all otolith types/sides), otolith area and perimeter were normalized to standard length of individuals prior to calculating aquarium means. This facilitated investigation of treatment effects while accounting for potentially confounding differences in standard length between fish. Next, each individual otolith was imaged with SEM in secondary electron mode using a working distance of 10 mm, spot size of 30, accelerating voltage of 10 kV, and magnification up to 3,000×. Scanning electron micrographs were scored visually for various mineralogy-related variables multiple times using Qualtrics survey software (Version N/A; https://www.qualtrics.com/). Six trained, independent readers scored variables including lateral development (scale of 1-5), crystal habit (orthorhombic, hexagonal, acicular, acrystalline, amorphous), percent visible crystals (5-50%), and mineralogy (proportion aragonite/vaterite on an otolith's surface interpretable by crystal habit) according to a rubric (see Supplemental Information 2 for the rubric used to train and guide readers through scoring<sup>1</sup>). The rubric contains reference illustrations (and in the case of the lateral development variable, micrographs) for each metric and lists categories to choose from for scoring; for each metric, the readers were asked to choose the option that best categorizes each otolith. Poor-quality micrographs due to mounting errors or broken otoliths were marked as unusable and not scored (41 micrographs, or roughly 4% of all micrographs, were excluded). Otolith-specific raw data grouped by type and side were generated for each variable from the survey questions. Each individual otolith was assigned the mode of survey scores for each variable. If a two-way mode tie occurred, the lower of the modes was selected. If a three-way mode tie occurred, the median mode was selected. For the lateral development and percent visible crystals variables, aquarium means were determined by calculating the arithmetic mean of the survey response mode for each otolith type and side, thus generating approximately continuous aquarium means from ordinal data (Norman, 2010). The mineralogy and crystal habit variables are nominal, so aquarium means were determined by calculating the mode of the otolith modes. See Data S1 for data means to be subset by otolith type/side and Data S2 for raw, fish-level data.

## Statistical analyses

Hypothesis tests were used to identify and interpret any impacts of increasing seawater pCO<sub>2</sub> on otolith morphology in each otolith type/side, as well as on fish mortality, settlement competency, and standard length. All statistical analyses were conducted using R (Version 3.4.3; R Core Team, 2017; see Supplemental information 1 for analyses). Regression analyses (pCO<sub>2</sub> as a continuous variable) were selected over ANOVA with multiple comparisons (pCO<sub>2</sub> as a grouping factor) for their greater power, informativeness, parsimony, and appropriateness for interpreting linear doseresponse relationships (Lazic, 2008). Polynomial models were considered for all regression analyses, and model selection performed using goodness of fit tests (i.e., F-tests for general linear models and chi-squared tests for generalized linear models). All binomial logistic regression models were tested for overdispersion. All statistical tests were two-tailed. The crystal habit and mineralogy response variables exhibited no variance across any treatment and otolith type, so they were excluded from further analyses. Principal component analysis (PCA) was performed on aquarium means for each otolith type and side. PCA was run on the correlation matrix between the morphometric (area, perimeter, circularity) and survey (lateral development, percent visible crystals) response variables using varimax rotation. Components with eigenvalues greater than or equal to 1.0 were retained. Treatment effects of pCO<sub>2</sub> on otolith morphometrics were investigated with regression analysis, with component scores as the response variables and pCO<sub>2</sub> as the explanatory variable. Regression analysis was performed on all components representing all otolith types and sides, and models in which pCO<sub>2</sub> predicted component scores (p < 0.05) were retained. Treatment effect on fish mortality was investigated with binomial logistic regression analysis (link function = logit), with the proportion of mortality counts (per aquarium)/aquarium stocking density as the response variable and pCO<sub>2</sub> as the explanatory variable. Treatment effect on somatic growth was investigated with regression analysis, with mean fish standard length (mm) as the response variable and pCO2 as the explanatory variable. Treatment effect on settlement competency at 10 dph was investigated with binomial logistic regression analysis, with the proportion of competent (per aquarium)/remaining fish (per aquarium) at the end of the experimental trial as the response variable and pCO2 as the explanatory variable. For all regression analyses that predicted an effect of pCO2, truncated models were created that are identical except that data from the 3,000 µatm pCO<sub>2</sub>/pH 7.30 treatment were excluded; this enabled interpretation of the models without the influence of this most extreme treatment, with the caveat that they employ n fewer degrees of freedom and are thus less powerful than the full models. For the truncated models, only F- and p-values are reported, as the full models were considered to be otherwise more informative.

# Results

# Seawater carbonate chemistry

pH treatments remained on target throughout the experimental trial (standard deviation  $\leq$  0.04) (Table 2).

Table 2: Seawater carbonate chemistry parameters.

Values represent aquaria means (n = 3 for each treatment); standard deviations listed in parentheses for measured parameters.

Treatment (pH <sub>T</sub> )	S (ppt)	T (°C)	A <sub>T</sub> (μmol kg <sup>-1</sup> )	DIC (µmol kg <sup>-1</sup> )	pCO <sub>2</sub> (µatm)	$\Omega_{Ar}$
8.16 (0.04)	35.00 (0.30)	28.20 (0.40)	2,440 (147)	2,018	299.4	4.84
7.80 (0.01)	35.00 (0.30)	28.20 (0.40)	2,440 (152)	2,237	825.5	2.54
7.60 (0.01)	35.00 (0.30)	28.30 (0.40)	2,432 (140)	2,318	1,384.3	1.70
7.30 (0.01)	35.00 (0.30)	28.20 (0.40)	2,418 (140)	2,415	2,897.0	0.89

DOI: 10.7717/peerj.6152/table-2

### **Otolith morphometrics and scoring**

Otolith morphometrics and mineralogical metrics varied with pCO<sub>2</sub> treatment and according to otolith type and side (Fig. 1). Scoring for the crystal habit and mineralogy metrics never deviated from the norm for any otolith type in any treatment (i.e., sagittae and lapilli were consistently

scored as predominantly aragonitic, exhibiting orthorhombic crystal habit; asterisci were assumed to be vateritic despite exhibiting little to no identifiable crystal habit).

### Mean Unstandardized Otolith Metrics

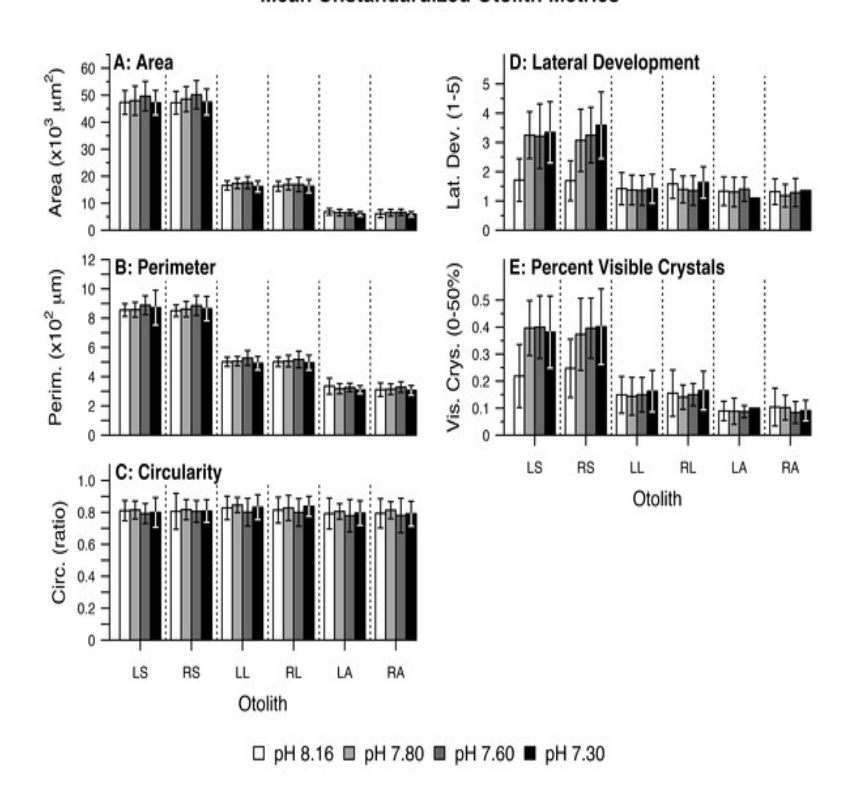


Figure 1: Mean unstandardized otolith metrics.

Summary of raw (fish-level) otolith morphological data including (A) Area, (B) Perimeter, (C) Circularity, (D) Lateral Development, and (E) Percent Visible Crystals by pH/pCO<sub>2</sub> treatment (legend) and otolith type/side. Otolith name abbreviations are identical to those elsewhere in the manuscript (e.g., LS for Left Sagittae). Bars represent combined means. Lines represent one (pooled) standard deviation.

DOI: 10.7717/peerj.6152/fig-1

# Principal component analysis

For each otolith type and side, principal component analysis produced two components with eigenvalues greater than 1.0 (Table 3). From here on, the components are referred to as rotated components—RC1 or RC2—to reflect that their loadings were scaled with varimax rotation. Left Sagittae (LS): As pCO<sub>2</sub> increased, left sagittae were rendered overall larger and wider in circumference, with more pronounced lateral faces and rougher surface textures owed to greater visible crystal density (Tables 3 and 4; Fig. 2A). Right Sagittae (RS): As pCO2 increased, right sagittae responded according to the same metrics as left sagittae, albeit with slightly stronger responses of area/SL and perimeter/SL (Tables 3 and 4; Fig. 2B). Whereas left sagittae responses were best represented as a linear model, right sagittae responses were best represented as a curvilinear (quadratic) model, with responses leveling out between the 1,600 µatm pCO<sub>2</sub>/pH 7.60 and 3,000 μatm pCO<sub>2</sub>/pH 7.30 treatments. Left lapilli (LL): As pCO<sub>2</sub> increased, left lapilli were rendered larger and wider in circumference (Tables 3 and 4; Fig. 2C). Right Lapilli (RL): In the most extreme pCO2 treatment only, right lapilli were rendered rougher with more pronounced lateral faces despite remaining approximately the same size (Tables 3 and 4; Fig. 2D). Whereas left lapilli responses were best represented as a curvilinear (quadratic) model, with responses leveling out between the 1,600 µatm pCO<sub>2</sub>/pH 7.60 and 3,000 µatm pCO<sub>2</sub>/pH 7.30 treatments, right lapilli responses were best represented as a linear model. Left Asterisci (LA): In the most extreme pCO<sub>2</sub> treatment only, left asterisci were rendered increasingly elliptical (rather than circular), rougher, and wider in circumference (Tables 3 and 4; Fig. 2E). This was the only instance of 2-dimensional otolith shape change observed in response to treatment, as well as the

only otolith metric that decreased rather than increased with increasing pCO<sub>2</sub>. *Right Asterisci* (*RA*): Right asterisci were not observed to respond to increasing pCO<sub>2</sub> (Fig. 2F). This was the only otolith type/side that exhibited no response to treatment.

Table 3:

Component variances and loadings.

Loadings corresponding to various Amphiprion *clarkii* otolith morphological parameters, the variance of which composes the rotated components in Fig. 2 and other components excluded from the analysis. Also included are the variances associated with each component and the total variance associated with components.

Otolith	Component	Variance (%)	Area/SL	Perimeter/SL	Circularity	Lateral development	Percent visible crystals
Left Sagittae	RC1 <sup>*</sup>	47	0.62*	0.37	0.05	0.97*	0.94*
3	RC2 Total	37 84	0.61	0.85	-0.86	0.08	0.17
Right Sagittae	RC1 <sup>*</sup>	59	0.77*	0.72*	0.00	0.95*	0.96*
3	RC2 Total	29 88	0.39	0.61	-0.94	0.06	-0.07
Left Lapilli	RC1	46	-0.12	-0.30	0.67	0.90	0.96
	RC2 <sup>*</sup> Total	36 82	0.89*	0.90*	-0.32	-0.29	-0.03
Right Lapilli	RC1	44	0.88	0.99	-0.65	-0.08	-0.01
	RC2 <sup>*</sup> Total	34 78	0.02	0.06	0.31	0.88*	0.92*
Left Asterisci	RC1	44	0.81	0.81	-0.15	-0.75	-0.54
	RC2 <sup>*</sup> Total	34 78	-0.11	0.53*	-0.92*	0.04	0.73*
Right Asterisci	RC1	50	0.89	0.98	-0.73	-0.06	0.48
	RC2 Total	24 74	-0.16	0.08	-0.31	0.91	0.50

DOI: 10.7717/peerj.6152/table-3

### Notes:

\*signify which components are related to pCO<sub>2</sub> (p < 0.05) and which variables are strongly associated with each of those components ( $r \ge 0.50$ ).

### Table 4:

Regression statistics.

Model	Comp.	DF	F	p	Equation	b <sub>1</sub> *100	CI*100	$R^2$
LS	RC1	1,10	11.98	0.0061	y = (7.28E-4)x - 0.98	0.07	0.03- 0.12	0.50
$LS_T$	RC1	1,7	10.67	0.0137	-	_	_	-
RS	RC1	2,9	20.56	0.0004	y = (2.51E-3)x - (5.08E-7)x <sup>2</sup> - 1.98)	-	-	0.78
$RS_T$	RC1	2,6	14.64	0.0049	-	_	_	-
LL	RC2	2,9	10.47	0.0045	y = (3.48E-3)x - $(8.86E - 7)x^2 - 2.25)$	-	-	0.63
$LL_T$	RC2	2,6	10.91	0.0100	_	_	_	_
RL	RC2	1,10	8.21	0.0168	y = (6.62E-4)x - 0.89	0.07	0.01- 0.12	0.40
$RL_T$	RC2	1,7	0.11	0.7489	_	_	_	_
LA	RC2	1,9	5.61	0.0420	y = (6.64E-4)x - 0.80	0.07	0.00- 0.13	0.32
$LA_T$	RC2	1,7	1.04	0.3423	_	_	_	_
FSC	-	1,10	4.83 <sup>a</sup>	0.0279	logit $(\pi) = (-3.81E-4)x + 2.31$	0.04	0.00- 0.07	0.38
$FSC_T$	_	1,7	7.26 <sup>a</sup>	0.0071	_	_	_	_
FSL	-	1,10	17.77	0.0018	y = (-1.31E-4)x + 6.85	0.01	0.00- 0.02	0.60
$FSL_T$	-	1,7	2.43	0.1629	-	-	-	-

DOI: 10.7717/peerj.6152/table-4

### **Notes:**

<sup>a</sup>For FSC and FSC<sub>T</sub>, which are binomial logistic regression models, the values listed as F are actually  $\chi^2$ -statistics.

### **Otolith Morphological Metrics**

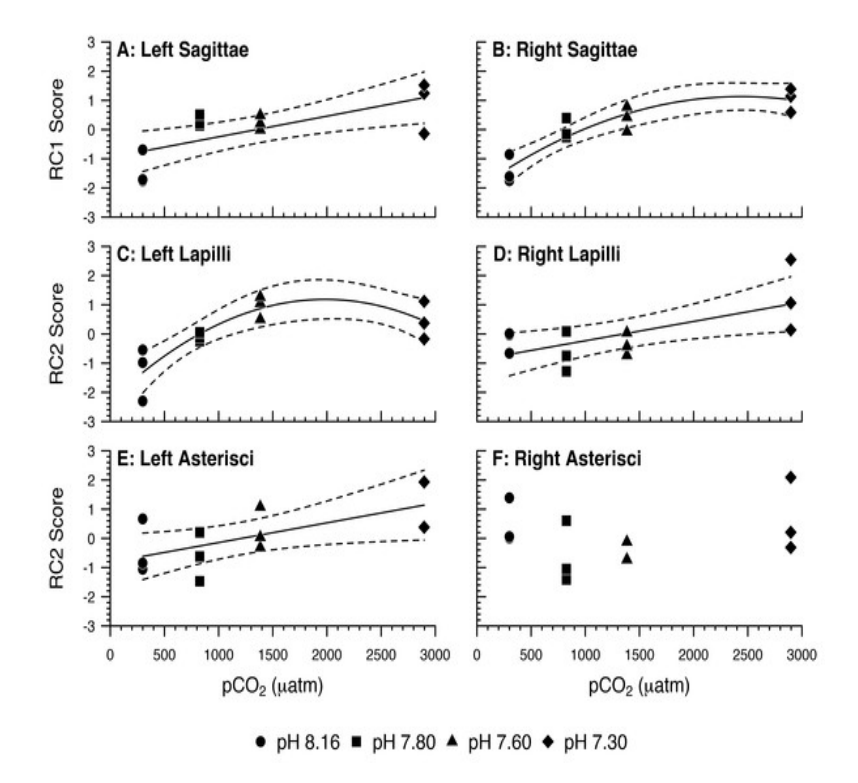


Figure 2: Otolith morphological metrics.

Regression lines (solid) and 95% confidence bands (dotted) represent significant relations between pH/pCO<sub>2</sub> treatment (legend) and (A, B, C, D, E) rotated component (RC) scores representing *Amphiprion clarkii* otolith morphological variables, grouped by otolith type and side (A, p=0.0061; B, p=0.0004; C, p=0.0045; D, p=0.0168; E, p=0.0420). Right asterisci components vs. pCO<sub>2</sub> did not yield significant relations, but RC2 scores are plotted for illustrative consistency. Data points represent aquaria. N=12, n=3 except where (E) no data is available for an aquarium (N=11, n=2 for pH 7.30 treatment only). See Table 3 for otolith morphological variables and corresponding PCA loadings.

DOI: 10.7717/peerj.6152/fig-2

# Mortality, settlement competency, and somatic growth:

Fish mortality, competency to settle at 10 dph, and standard length varied somewhat with pCO<sub>2</sub> treatment (Fig. 3). Despite high fish mortality throughout the experimental trial, mortality was not associated with pCO<sub>2</sub> (Table 4, Fig. 4A). As pCO<sub>2</sub> increased, fewer fish were competent to settle at 10 dph (Table 4, Fig. 4B). In the most extreme pCO<sub>2</sub> treatment only, fish exhibited diminished somatic growth relative to those at lower concentrations (Fig. 4C).

# **Mean Fish Condition Metrics**

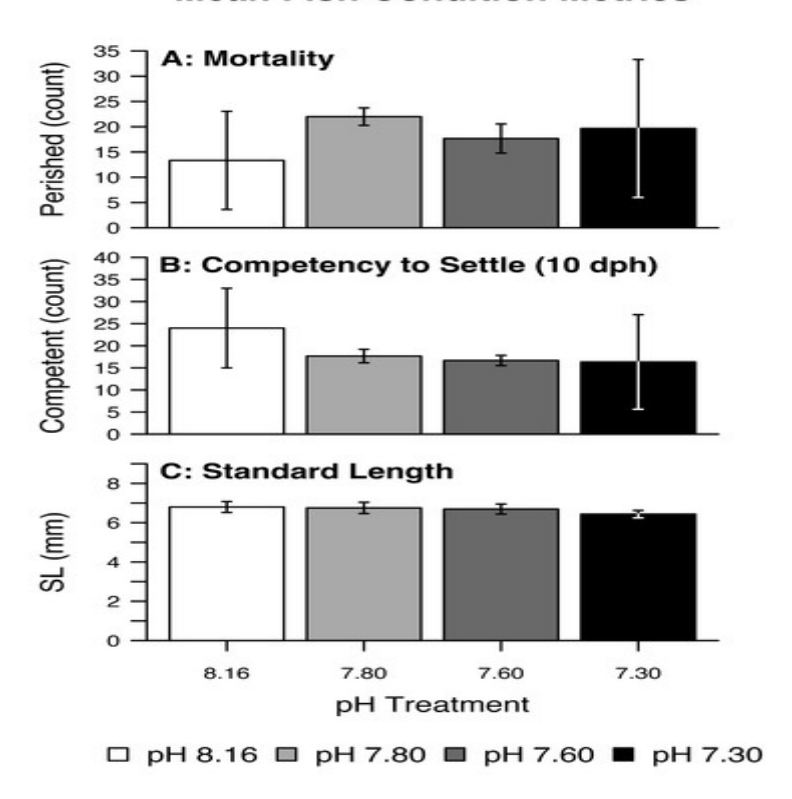


Figure 3: Mean fish condition metrics.

Summary of raw (fish-level) fish condition data by pH/pCO $_2$  treatment (legend) including (A) Mortality, (B) Competency to Settle at 10 days post-hatch (dph), (C) Standard Length. Bars represent combined means. Lines represent one (pooled) standard deviation.

DOI: 10.7717/peerj.6152/fig-3

### **Fish Condition Metrics**

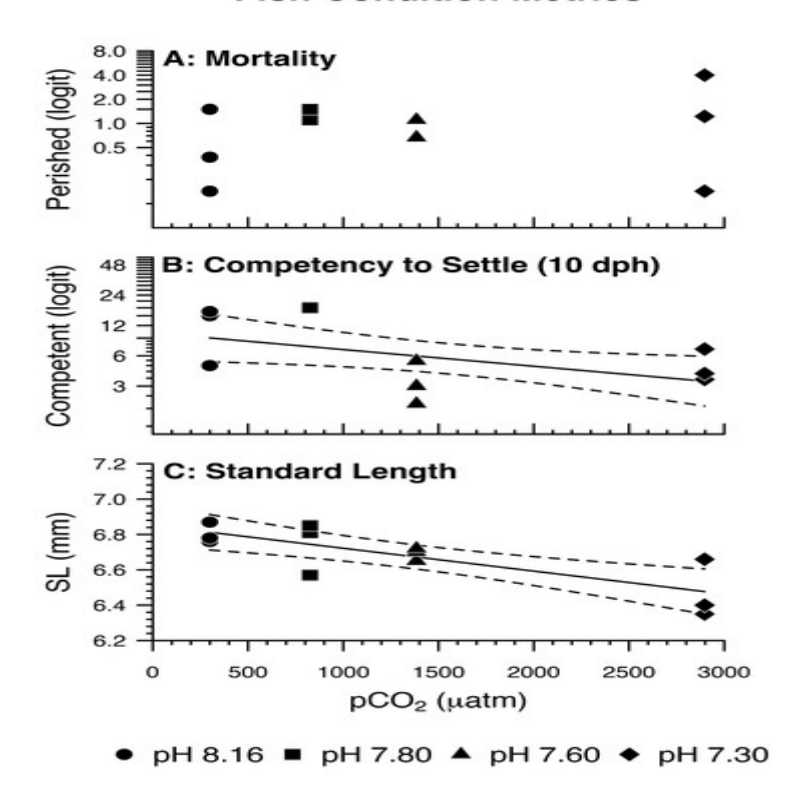


Figure 4: Fish condition metrics.

(A) Odds of *Amphiprion clarkii* mortality by pH/pCO<sub>2</sub> treatment (legend). Regression lines (solid) and 95% confidence bands (dotted) represent significant relations between pH/pCO<sub>2</sub> treatment and (B) odds of on-time *A. clarkii* settlement (p = 0.0279); (C) *A. clarkii* standard length (p = 0.0018). Data points represent (A, B) binomial proportions by aquarium; (C) aquarium means. N = 12, n = 3 except where (B) 100% of fish in an aquarium settled on time (N = 10, N = 1 for pH 7.80 treatment only).

DOI: 10.7717/peerj.6152/fig-4

# **Discussion**

Otoliths exhibited diverse responses to treatment according to type and side. In response to increasing seawater pCO<sub>2</sub>, all three otolith types exhibited increasing perimeter and percent visible crystals, sagittae and lapilli exhibited increasing area and lateral development, and asterisci exhibited differences in shape. While the sagittae changed according to the same metrics regardless of side, the lapilli and asterisci changed according to different metrics depending on side. These differences reveal important things about the nature of the metrics under investigation; for example, while both sagittae responded to treatment by growing larger with more pronounced lateral faces, these effects were segregated according to side in the lapilli; this suggests that otolith area and lateral development are uncoupled rather than being two immutably conjoined metrics of growth. As such, it is often informative to investigate each otolith independently rather than investigating one type or pooling by type without regard to side. Among the 24 studies reviewed here that analyzed ocean acidification impacts on otolith morphology, five investigated lapilli (Table 1), none investigated asterisci, and eight segregated otoliths by side during morphometric analysis (at least six of which pooled them after observing no evidence of asymmetry) (Franke & Clemmesen, 2011; Munday et al., 2011a; Munday et al., 2011b; Maneja et al., 2013; Bignami, Sponaugle & Cowen, 2014; Mu et al., 2015; Perry et al., 2015; Réveillac et al., 2015; Martins, 2017; Jarrold & Munday, 2018). However, the results suggest that responses of one or two otoliths cannot necessarily be extrapolated to the rest of the otolith system.

Some regression models were disproportionately weighted by the 3,000  $\mu$ atm pCO<sub>2</sub>/pH 7.30 treatment, as evidenced by the *p*-value change between the full model and truncated model with data from that treatment excluded. Although the *p*-values for all otolith morphological models increased with truncation (Table 4, attributable in part to a loss of power from fewer degrees of freedom), the p-values for the right lapilli and left asterisci models rose >0.05, indicating there is

little to no evidence of pCO<sub>2</sub> impacts on those otoliths except in conditions of aragonite undersaturation. For the lapilli, this exercise indicates an asymmetry of resilience: left lapilli are impacted by lower pCO<sub>2</sub> concentrations, whereas right lapilli are not. Nevertheless, this still results in morphological asymmetry of lapilli at lower concentrations. For the asterisci, it indicates mutual resilience at lower concentrations, and morphological asymmetry at the highest concentration. Scenarios in which these relationships are ecologically relevant could include isolated coastal systems with poor mixing under additional pressure from eutrophication (Wallace et al., 2014; Fabricius, 2005) or volcanism (Vogel et al., 2015). However, lower concentrations are here considered more typical of the future ocean.

Researchers previously examined otolith development in teleost larvae reared under acidified conditions, and despite differences in methodology and model species, it is possible to draw comparisons. Notably, Munday et al. (2011b)'s study species (*Amphiprion percula*) enables intragenus comparison with *A. clarkii*. Here, the results are consistent with those of Munday et al. (2011b) and several others (Table 1) in that sagittae grew at elevated seawater pCO<sub>2</sub>. However, Munday et al. (2011b) observed growth in left sagittae only, whereas *A. clarkii* exhibited growth in both sagittae. The results are further consistent with six of those studies (Table 1) in that lapilli also grew at elevated pCO<sub>2</sub> (albeit in the left ear only). Regarding otolith shape: the results are consistent with five studies (Table 1) in that otolith shape changed at elevated pCO<sub>2</sub>, albeit in left asterisci only, and only in conditions of aragonite undersaturation. A caveat: whereas most other studies reared fish from two or more genotypes (e.g., Munday et al., 2011a; Munday et al., 2011b; Bignami, Sponaugle & Cowen, 2013; Bignami et al., 2013; Bignami, Sponaugle & Cowen, 2014), the present study used one clutch of eggs produced by one broodstock pair. While this eliminated lineage as a potentially confounding variable in the analysis, care should be taken when comparing the results of this study with others or extrapolating to larger populations.

Some of the observed effects of seawater pCO<sub>2</sub> on otolith growth in *A. clarkii*, including increasing area, perimeter, and lateral development, may be consequences of acid-base regulation triggered by respiratory acidosis. Fishes normalize internal pH disturbances by metabolic adjustment: blood plasma  $HCO_3^-$  is absorbed/retained and  $H^+$  excreted by modulating rates of transport across the gill epithelium. However, extracellular pCO<sub>2</sub> and  $HCO_3^-$  remain elevated following pH adjustment, and excess  $HCO_3^-$  is imported to the endolymph where it becomes substrate for  $CO_3^{2-}$  aggregation, enhancing net otolith calcification (Checkley et al., 2009; Munday et al., 2011b; Heuer & Grosell, 2014).

Since otoliths are critical components of the ears and vestibular organs (Fekete, 2003; Moyle & Cech, 2004), ocean acidification-driven changes to otolith development may challenge sensory perception in A. clarkii and other teleosts (e.g., Munday et al., 2011b; Bignami et al., 2013; Bignami, Sponaugle & Cowen, 2014). Indeed, there is some empirical evidence outside the context of ocean acidification that marine fish exhibiting abnormal otolith morphology or asymmetry suffer diminished sensory ability. In terms of hearing, fish with larger, vateritic, and/or otherwise asymmetrical sagittae exhibited reduced sensitivity or deafness (Oxman et al., 2007; Gagliano et al., 2008; Browning et al., 2012); some presumably because vaterite is less dense than aragonite, thereby reducing otolith displacement amplitude and effectiveness in the inner ear (Bignami et al., 2013; Reimer et al., 2016). Although there remains no evidence of ocean acidification-induced vaterite replacement in otoliths, including in A. clarkii, there is some evidence for calcite replacement in sagittae and lapilli at elevated pCO<sub>2</sub> (Coll-Lladó et al., 2018); calcite is similarly less dense than aragonite (Nakamura Filho et al., 2014). In terms of kinesthesia, some fish with abnormal and/or asymmetric sagittae/lapilli exhibited kinetoses (Söllner, 2003; Anken, Knie & Hilbig, 2017); however, other studies observed pCO<sub>2</sub> impacts on otolith morphology without observing impacts on behavior (Bignami, Sponaugle & Cowen, 2013; Bignami, Sponaugle & Cowen, 2014; Shen et al., 2016). It is possible the pCO2 impacts on otolith morphology and asymmetry observed here could impair A. clarkii hearing and kinesthesia, but no sensory or behavioral assays were conducted, so hypotheses remain speculative.

In addition to corroborating reports of otolith growth along the x and y axes (i.e., increasing area and perimeter) in young teleosts in response to increasing seawater pCO<sub>2</sub>, there was evidence for pCO<sub>2</sub>-induced otolith growth along the z-axis (i.e., upward growth from the lateral face) in A. clarkii. Lateral development appears most conspicuous in sagittae, and linked to treatment in sagittae and right lapilli, although it was observable in asterisci as well. While lateral development occurs on the lateral face, which does not directly interact with maculae, it is possible this CaCO<sub>3</sub> aggregation will increase otolith mass at a magnitude greater than that which is evident from increased 2-dimensional area and perimeter. Thus, sagittae exhibiting advanced lateral development may have a wider displacement amplitude independent of area and perimeter, enhancing auditory sensitivity (Bignami et al., 2013); however, displacement amplitude was not measured here. This hypothesis is independent of otolith composition, for which there was no evidence of having changed, but which undermined auditory sensitivity in some studies (Oxman et al., 2007; Browning et al., 2012; Reimer et al., 2016). Also, since lateral development appears

to occur on only one face of the otolith (though the medial face was not investigated here, all otoliths were imaged convex-side up, which was invariably the lateral face), its center of mass likely changed as well, with unknown consequences for otic mechanics.

Some of the otoliths appear visibly smooth on the surface, while others appear rougher due to the exposure of aragonite table edges and similar crystal activity. Estimating percent visible crystals is akin to estimating otolith surface roughness. The observation that percent visible crystals increased with increasing pCO<sub>2</sub> in sagittae, right lapilli, and left asterisci is consistent with the characterization of rough-type otoliths as abnormal in other species (Béarez et al., 2005; Ma et al., 2008; Browning et al., 2012). Increasing roughness could be a symptom of haphazard CaCO<sub>3</sub> aggregation, evidence of altered protein matrix deposition, and/or a snapshot of an evolving CaCO<sub>3</sub> crystal habit/polymorph baseline. While increasing roughness seems unlikely to affect otolith displacement amplitude, it could conceivably impact otolith-maculae mechanics with unknown consequences for function; in some fish, otoliths are observed to be rough on the ventral end only, driving maculae deformation by hooking them to the otolith surface (Ohnishi et al., 2002). More research concurrently investigating fish behavior, ocean acidification-induced otolith roughness, and maculae displacement is needed to explore this hypothesis.

As might be expected when rearing many hundreds of fish in the most delicate early stages of development, Amphiprion clarkii larvae experienced substantial mortality throughout the experimental trial. Although there is evidence in the literature of acute CO2 toxicity in larval teleosts, this is typically observed at pCO<sub>2</sub> levels far exceeding those evaluated here (i.e., >48,000 uatm) (Kikkawa, Ishimatsu & Kita, 2003; Ishimatsu et al., 2004; Kikkawa, Kita & Ishimatsu, 2004); this is consistent with the absence of evidence that treatment instigated fish mortality. The sublethal impact of pCO<sub>2</sub> on settlement competency at 10 dph, however, was dramatic. There is some evidence of inhibited larval growth following delays in metamorphosis (Victor, 1986; McCormick, 1999), and some degree of inhibited growth was observed here, but the present analysis should be interpreted with caution due to the following caveats: (i) 10 dph was selected as the onset of metamorphosis and presumed settlement competency, but this threshold may be arbitrary to metamorphosis and settlement completion; (ii) metamorphosis and response to settlement cues may decouple at elevated seawater pCO<sub>2</sub> (Rossi et al., 2015), complicating metamorphosis as a reliable indicator for settlement competency; (iii) indeed, laboratory-reared fish were unexposed to settlement cues including reef sounds, lunar phase, and anemone presence; (iv) otolith microstructure evidence of settlement competency was not investigated; (v) inhibited larval growth due to delayed metamorphosis isn't known to translate to inhibited growth post-settlement (McCormick, 1999). Finally, the impact on somatic growth was marginal: the reduction in fish standard lengths with increasing pCO2 amounts to a small fraction of fish standard lengths, and this effect was only relevant in conditions of aragonite undersaturation.

# **Conclusions**

This work corroborates evidence of otolith growth and altered shape with increasing seawater pCO<sub>2</sub> reported for other taxa in a novel taxon, *Amphiprion clarkii*. In addition, it reports evidence of increasing otolith lateral development and surface roughness with increasing pCO<sub>2</sub>. Impacts were observed in all otolith types, including the previously uninvestigated asterisci. Each otolith type and side were investigated independently, indicating asymmetrical responses of lapilli and asterisci to pCO<sub>2</sub>. The experimental design and analysis facilitated construction of pCO<sub>2</sub> doseresponse curves, which were created for all otolith types and sides in *A. clarkii* excepting right asterisci. These curves outline changes to multiple morphometric and mineralogical variables and may be leveraged to predict responses to pCO<sub>2</sub> conditions not investigated here. These responses could impact auditory and/or vestibular sensitivity in teleosts, adding to previous observations and hypotheses involving sagittae and lapilli. In summary, the work adds to the existing knowledge base regarding otolith response to ocean acidification, which may aid in predicting and preserving teleost fitness in the near-future ocean.

# **Supplemental Information**

# **Additional Information and Declarations**

### **Competing Interests**

The authors declare there are no competing interests.

# **Author Contributions**

Robert J. Holmberg, Alan Stebbins, Steven W. Nye Jr., Aaron Honig, Amy E. Johnston, and Christine M. San Antonio analyzed the data, prepared figures and/or tables, authored or reviewed drafts of the paper, approved the final draft.

Eric Wilcox-Freeburg conceived and designed the experiments, performed the experiments, analyzed the data, authored or reviewed drafts of the paper, approved the final draft.

Andrew L. Rhyne conceived and designed the experiments, performed the experiments, analyzed the data, contributed reagents/materials/analysis tools, authored or reviewed drafts of the paper, approved the final draft.

Michael F. Tlusty and Robyn E. Hannigan conceived and designed the experiments, analyzed the data, contributed reagents/materials/analysis tools, prepared figures and/or tables, authored or reviewed drafts of the paper, approved the final draft.

Bradford Bourque conceived and designed the experiments, performed the experiments, contributed reagents/materials/analysis tools, authored or reviewed drafts of the paper, approved the final draft.

### **Animal Ethics**

The following information was supplied relating to ethical approvals (i.e., approving body and any reference numbers):

IACUC at Roger Williams University in Bristol, Rhode Island provided full approval for this research (IACUC #R-11-09-13).

## **Data Availability**

The following information was supplied regarding data availability:

Raw data are provided in the Supplemental Material;

BCO-DMO (OA-OTO MIN; https://www.bco-dmo.org/project/2240); and GitHub (https://github.com/edfreeburg/RSS-feed-DigitalAquaticsRKE/blob/master/DA\_RSS\_Multiple.pl; https://github.com/edfreeburg/RSS-feed-DigitalAquaticsRKE/blob/master/rss\_data.m; https://github.com/edfreeburg/MATLAB-Image-Analysis/blob/master/Morpho.m).

### **Funding**

This study was supported by grants from the National Science Foundation [NSF-CRI-OA-1220480 (PIs: Hannigan, Tlusty, Rhyne)] and the National Science Foundation Rhode Island Experimental Program to Stimulate Competitive Research [EPSCoR-RI (PI: Rhyne)]. The funders had no role in study design, data collection and analysis, decision to publish, or preparation of the manuscript.

The authors would like to acknowledge Bill Robinson, Meng Zhou, Solange Brault, and Gene Gallagher for advice and guidance; Bryanna Broadaway, Alex Eisen-Cuadra, Ashley Bulseco-McKim, Jeremy Williams, Katie Flanders, and Nicole Henderson for assistance and support; and undergraduates from Roger Williams University who assisted with the experimental trial and data collection: Kristen Kiefer, Shawna Chamberlin, Jackie Mitchell, Drew Canfield, Allex Gourlay, and Matt Muscara.

# References

Anken R, Knie M, Hilbig R. 2017. Inner ear otolith asymmetry in late-larval cichlid fish (Oreochromis mossambicus, Perciformes) showing kinetotic behaviour under diminished gravity. Scientific Reports 7:15630

Béarez P, Carlier G, Lorand JP, Parodi GC. 2005. Destructive and non-destructive microanalysis of biocarbonates applied to anomalous otoliths of archaeological and modern sciaenids (Teleostei) from Peru and Chile. Comptes Rendus Biologies 328:243-252

**Bell PRF, Elmetri I, Lapointe BE. 2014.** Evidence of large-scale chronic eutrophication in the Great Barrier Reef: quantification of chlorophyll a thresholds for sustaining coral reef communities. Ambio **43**:361-376

**Bignami S, Enochs IC, Manzello DP, Sponaugle S, Cowen RK. 2013**. Ocean acidification alters the otoliths of a pantropical fish species with implications for sensory function. Proceedings of the National Academy of Sciences of the United States of America 110:7366-7370

**Bignami S, Sponaugle S, Cowen RK. 2013**. Response to ocean acidification in larvae of a large tropical marine fish, Rachycentron canadum. Global Change Biology **19**:996-1006

Bignami S, Sponaugle S, Cowen RK. 2014. Effects of ocean acidification on the larvae of a high-value pelagic fisheries species, Mahi-mahi Coryphaena hippurus. Aquatic Biology 21:249-260

Boulos RA, Zhang F, Tjandra ES, Martin AD, Spagnoli D, Raston CL. 2015. Spinning up the polymorphs of calcium carbonate. Scientific Reports 4:3616

Browning ZS, Wilkes AA, Moore EJ, Lancon TW, Clubb FJ. 2012. The effect of otolith malformation on behavior and cortisol levels in juvenile red drum fish (Sciaenops ocellatus) CompMed 62:251-256

Byrne RH. 1987. Standardization of standard buffers by visible spectrometry. Analytical Chemistry 59:1479-1481

Caldeira K, Wickett ME. 2003. Oceanography: anthropogenic carbon and ocean pH. Nature 425:365

Cattano C, Calò A, Di Franco A, Firmamento R, Quattrocchi F, Sdiri K, Guidetti P, Milazzo M. 2017. Ocean acidification does not impair predator recognition but increases juvenile growth in a temperate wrasse off CO<sub>2</sub> seeps. Marine Environmental Research 132:33-40

Checkley DM, Dickson AG, Takahashi M, Radich JA, Eisenkolb N, Asch R. 2009. *Elevated CO*<sub>2</sub> enhances otolith growth in young fish. Science **324**:1683

Coll-Lladó C, Giebichenstein J, Webb PB, Bridges CR, De La Serrana DG. 2018. Ocean acidification promotes otolith growth and calcite deposition in gilthead sea bream (Sparus aurata) larvae. Scientific Reports 8:1-10

**Doney SC, Fabry VJ, Feely RA, Kleypas JA. 2009**. *Ocean acidification: the other CO<sub>2</sub> problem*. Annual Review of Marine Science 1:169-192

**Esbaugh AJ, Heuer R, Grosell M. 2012.** *Impacts of ocean acidification on respiratory gas exchange and acid-base balance in a marine teleost, Opsanus beta.* Journal of Comparative Physiology B: Biochemical, Systemic, and Environmental Physiology **182**:921-934

Fabricius KE. 2005. Effects of terrestrial runoff on the ecology of corals and coral reefs: review and synthesis. Marine Pollution Bulletin 50:125-146

Fabry VJ, Seibel BA, Feely RA, Fabry JCO, Fabry VJ. 2008. Impacts of ocean acidification on marine fauna and ecosystem processes. ICES Journal of Marine Science 65:414-432

Faria AM, Filipe S, Lopes AF, Oliveira AP, Gonçalves EJ, Ribeiro L. 2017. Effects of high pCO<sub>2</sub> on early life development of pelagic spawning marine fish. Marine and Freshwater Research 68:2106-2114

Fekete DM. 2003. Rocks that roll zebrafish. Science 302:241-242

Franke A, Clemmesen C. 2011. Effect of ocean acidification on early life stages of Atlantic herring (Clupea harengus L.) Biogeosciences 8:3697-3707

Froese R, Pauly D. 2018. Fishbase. FishBase.

Frommel AY, Schubert A, Piatkowski U, Clemmesen C. 2013. Egg and early larval stages of Baltic cod, Gadus morhua, are robust to high levels of ocean acidification. Marine Biology 160:1825-1834

Gagliano M, Depczynski M, Simpson SD, Moore JA. 2008. Dispersal without errors: symmetrical ears tune into the right frequency for survival. Proceedings of the Royal Society B: Biological Sciences 275:527-534

Gattuso J, Buddemeier RW. 2000. Calcification and CO<sub>2</sub>. Nature 407:311-313

Gaylord B, Kroeker KJ, Sunday JM, Anderson KM, Barry JP, Brown NE, Connell SD, Dupont S, Fabricius KE, Hall-Spencer JM+10 more. 2015. Ocean acidification through the lens of ecological theory. Ecology 96:3-15

**Grosell M. 2011**. Intestinal anion exchange in marine teleosts is involved in osmoregulation and contributes to the oceanic inorganic carbon cycle. Acta Physiologica **202**:421-434

Hendriks IE, Duarte CM, Álvarez M. 2010. Vulnerability of marine biodiversity to ocean acidification: a meta-analysis. Estuarine, Coastal and Shelf Science 86:157-164

**Heuer RM, Grosell M. 2014.** *Physiological impacts of elevated carbon dioxide and ocean acidification on fish.* American Journal of Physiology-Regulatory, Integrative and Comparative Physiology **307**:R1061-R1084

Hoegh-Guldberg O, Poloczanska ES, Skirving W, Dove S. 2017. Coral reef ecosystems under climate change and ocean acidification. Frontiers in Marine Science 4:158

Hurst TP, Fernandez ER, Mathis JT, Miller JA, Stinson CM, Ahgeak EF. 2012. Resiliency of juvenile walleye pollock to projected levels of ocean acidification. Aquatic Biology 17:247-259

**IPCC. 2013**. Climate change 2013: the physical science basis. Contribution of working group I to the Fifth Assessment Report of the Intergovernmental Panel on Climate Change. Stocker TF, Qin D, Plattner G-K, Tignor M, Allen SK, Boschung J, Nauels A, Xia Y, VB, PMM

Ishimatsu A, Hayashi M, Kikkawa T. 2008. Fishes in high-CO<sub>2</sub>, acidified oceans. Marine Ecology Progress Series 373:295-302

Ishimatsu A, Kikkawa T, Hayashi M, Lee K-S, Kita J. 2004. Effects of CO<sub>2</sub> on marine fish: larvae and adults. Journal of Oceanography 60:731-741

**Jarrold MD, Munday PL. 2018**. Diel CO<sub>2</sub> cycles do not modify juvenile growth, survival and otolith development in two coral reef fish under ocean acidification. Marine Biology **165**:1-12

Kikkawa T, Ishimatsu A, Kita J. 2003. Acute CO<sub>2</sub> tolerance during the early developmental stages of four marine teleosts. Environmental Toxicology 18:375-382

Kikkawa T, Kita J, Ishimatsu A. 2004. Comparison of the lethal effect of CO<sub>2</sub> and acidification on red sea bream (Pagrus major) during the early developmental stages. Marine Pollution Bulletin 48:108-110

Kroeker KJ, Kordas RL, Crim R, Hendriks IE, Ramajo L, Singh GS, Duarte CM, Gattuso JP. 2013. *Impacts of ocean acidification on marine organisms: quantifying sensitivities and interaction with warming.* Global Change Biology **19**:1884-1896

Kroeker KJ, Micheli F, Gambi MC. 2012. Ocean acidification causes ecosystem shifts via altered competitive interactions. Nature Climate Change 3:156-159

- **Lazic SE. 2008.** Why we should use simpler models if the data allow this: relevance for ANOVA designs in experimental biology. BMC Physiology 8:1-7
- Le Quéré C, Takahashi T, Buitenhuis ET, Rödenbeck C, Sutherland SC. 2010. Impact of climate change and variability on the global oceanic sink of CO<sub>2</sub>. Global Biogeochemical Cycles 24:n/a
- Lychakov DV, Rebane YT. 2005. Fish otolith mass asymmetry: morphometry and influence on acoustic functionality. Hearing Research 201:55-69
- Ma T, Kuroki M, Miller MJ, Ishida R, Tsukamoto K. 2008. Morphology and microchemistry of abnormal otoliths in the ayu, Plecoglossus altivelis. Environmental Biology of Fishes 83:155-167
- Maneja RH, Frommel AY, Geffen AJ, Folkvord A, Piatkowski U, Chang MY, Clemmesen C. 2013. Effects of ocean acidification on the calcification of otoliths of larval Atlantic cod Gadus morhua. Marine Ecology Progress Series 477:251-258
- Martino J, Doubleday ZA, Woodcock SH, Gillanders BM. 2017. Elevated carbon dioxide and temperature affects otolith development, but not chemistry, in a diadromous fish. Journal of Experimental Marine Biology and Ecology 495:57-64
- Martins SIG. 2017. Impacts of CO<sub>2</sub>-induced ocean acidification on predator detection ability and developement of temperate fish. PhD thesis, ISPA—Instituto Universitário de Ciências Psicológicas, Sociais e da Vida, Lisboa, Portugal thesis
- McCormick MI. 1999. Delayed metamorphosis of a tropical reef fish (Acanthurus triostegus): a field experiment. Marine Ecology Progress Series 176:25-38
- Mikaloff Fletcher SE, Gruber N, Jacobson AR, Doney SC, Dutkiewicz S, Gerber M, Follows M, Joos F, Lindsay K, Menemenlis D+3 more. 2006. Inverse estimates of anthropogenic CO<sub>2</sub> uptake, transport, and storage by the ocean. Global Biogeochemical Cycles 20:1-16
- Millero FJ, Zhang JZ, Fiol S, Sotolongo S, Roy RN, Lee K, Mane S. 1993. The use of buffers to measure the pH of seawater. Marine Chemistry 44:143-152
- Mirasole A, Gillanders BM, Reis-Santos P, Grassa F, Capasso G, Scopelliti G, Mazzola A, Vizzini S. **2017**. The influence of high  $pCO_2$  on otolith shape, chemical and carbon isotope composition of six coastal fish species in a Mediterranean shallow  $CO_2$  vent. Marine Biology **164**:1-15
- **Moyle PB, Cech JJ. 2004**. Lee C, ed. Fishes, an introduction to ichtyology (5th ed). San Francisco: Pearson Benjamin Cummings.
- Mu J, Jin F, Wang J, Zheng N, Cong Y, Wang JY. 2015. Effects of CO<sub>2</sub>-driven ocean acidification on early life stages of marine medaka (Oryzias melastigma) Biogeosciences 12:3861-3868
- Munday PL, Crawley NE, Nilsson GE. 2009. Interacting effects of elevated temperature and ocean acidification on the aerobic performance of coral reef fishes. Marine Ecology Progress Series 388:235-242
- Munday PL, Gagliano M, Donelson JM, Dixson DL, Thorrold SR. 2011a. Ocean acidification does not affect the early life history development of a tropical marine fish. Marine Ecology Progress Series 423:211-221
- Munday PL, Hernaman V, Dixson DL, Thorrold SR. 2011b. Effect of ocean acidification on otolith development in larvae of a tropical marine fish. Biogeosciences 8:1631-1641
- Munday PL, Jones GP, Pratchett MS, Williams AJ. 2008. Climate change and the future for coral reef fishes. Fish and Fisheries 9:261-285
- Nakamura Filho A, De Almeida AC, Riera HE, De Araújo JLF, Gouveia VJP, De Carvalho MD, Cardoso AV. 2014. Polymorphism of CaCO<sub>3</sub> and microstructure of the shell of a Brazilian invasive mollusc (Limnoperna fortunei) Materials Research Bulletin 17:15-22
- Nilsson GE, Dixson DL, Domenici P, McCormick MI, Sørensen C, Watson S-A, Munday PL. 2012. Near-future carbon dioxide levels alter fish behaviour by interfering with neurotransmitter function. Nature Climate Change 2:201-204
- Norman G. 2010. Likert scales, levels of measurement and the "laws" of statistics. Advances in Health Sciences Education 15:625-632
- Ohnishi K, Yamamoto T, Ogawa Y, Takahashi A, Yamashita M, Ohnishi T. 2002. High transmittance of X-rays in the utricular otolith of upside-down swimming catfish, Synodontis nigriventris. Biological Sciences in Space 16:18-21
- Orr JC, Fabry VJ, Aumont O, Bopp L, Doney SC, Feely RA, Gnanadesikan A, Gruber N, Ishida A, Joos F+17 more. 2005. Anthropogenic ocean acidification over the twenty-first century and its impact on calcifying organisms. Nature 437:681-686
- Oxman DS, Barnett-Johnson R, Smith ME, Coffin A, Miller DL, Josephson R, Popper AN. 2007. The effect of vaterite deposition on sound reception, ototlith morphology, and inner ear sensory epithelia in hatchery-reared chinook salmon (Oncorhynchus tshawytscha) Canadian Journal of Fisheries and Aquatic Sciences 64:1469-1478
- Panella G. 1971. Fish otoliths: daily growth layers and periodical patterns. Science 173:1124-1127
- Perry DM, Redman DH, Widman JC, Meseck S, King A, Pereira JJ. 2015. Effect of ocean acidification on growth and otolith condition of juvenile scup, Stenotomus chrysops. Ecology and Evolution 5:4187-4196
- Pimentel MS, Faleiro F, Dionisio G, Repolho T, Pousao-Ferreira P, Machado J, Rosa R. 2014. Defective skeletogenesis and oversized otoliths in fish early stages in a changing ocean. Journal of Experimental Biology 217:2062-2070

**Popper AN, Fay RR. 1993**. Sound detection and processing by fish: critical review and major research questions. Brain Behavior and Evolution **41**:14-25

Queirós AM, Fernandes JA, Faulwetter S, Nunes J, Rastrick SPS, Mieszkowska N, Artioli Y, Yool A, Calosi P, Arvanitidis C+4 more. 2015. Scaling up experimental ocean acidification and warming research: from individuals to the ecosystem. Global Change Biology 21:130-143

R Core Team. 2017. R: a language and environment for statistical computing. Version 3.4.3 Vienna: R Foundation for Statistical Computing. software

Reimer T, Dempster T, Warren-Myers F, Jensen AJ, Swearer SE. 2016. High prevalence of vaterite in sagittal otoliths causes hearing impairment in farmed fish. Scientific Reports 6:25249

Réveillac E, Lacoue-Labarthe T, Oberhänsli F, Teyssié JL, Jeffree R, Gattuso JP, Martin S. 2015. *Ocean acidification reshapes the otolith-body allometry of growth in juvenile sea bream.* Journal of Experimental Marine Biology and Ecology 463:87-94

Ries JB, Cohen AL, McCorkle DC. 2009. Marine calcifiers exhibit mixed responses to CO<sub>2</sub>-induced ocean acidification. Geology 37:1131-1134

Rossi T, Nagelkerken I, Simpson SD, Pistevos JCA, Watson S-A, Merillet L, Fraser P, Munday PL, Connell SD. 2015. Ocean acidification boosts larval fish development but reduces the window of opportunity for successful settlement. Proceedings of the Royal Society B: Biological Sciences 282:20151954

Schade FM, Clemmesen C, Wegner KM. 2014. Within- and transgenerational effects of ocean acidification on life history of marine three-spined stickleback (Gasterosteus aculeatus) Marine Biology 161:1667-1676

Seibel BA, Maas AE, Dierssen HM. 2012. Energetic plasticity underlies a variable response to ocean acidification in the pteropod, Limacina helicina antarctica. PLOS ONE 7:e30464

Shen SG, Chen F, Schoppik DE, Checkley DM. 2016. Otolith size and the vestibulo-ocular reflex of larvae of white seabass Atractoscion nobilis at high pCO<sub>2</sub>. Marine Ecology Progress Series 553:173-182

Simpson SD, Munday PL, Wittenrich ML, Manassa R, Dixson DL, Gagliano M, Yan HY. 2011. Ocean acidification erodes crucial auditory behaviour in a marine fish. Biology Letters 7:917-920

Söllner C. 2003. Control of crystal size and lattice formation by starmaker in otolith biomineralization. Science 302:282-286

Victor BC. 1986. Delayed metamorphosis with reduced larval growth in a coral reef fish (Thalassoma bifasciatum) Canadian Journal of Fisheries and Aquatic Sciences 43:1208-1213

Vogel N, Fabricius KE, Strahl J, Noonan SHC, Wild C, Uthicke S. 2015. Calcareous green alga Halimeda tolerates ocean acidification conditions at tropical carbon dioxide seeps. Limnology and Oceanography 60:263-275

Wallace RB, Baumann H, Grear JS, Aller RC, Gobler CJ. 2014. Coastal ocean acidification: the other eutrophication problem. Estuarine, Coastal and Shelf Science 148:1-13

Wilcox-Freeburg ED. 2014. Exploring the link between otolith growth and function along the biological continuum in the context of ocean acidification. PhD thesis, University of Massachusetts Boston, Boston, MA thesis

Wilcox-Freeburg E, Rhyne A, Robinson WE, Tlusty M, Bourque B, Hannigan RE. 2013. A comparison of two pH-stat carbon dioxide dosing systems for ocean acidification experiments. Limnology and Oceanography: Methods 11:485-494

### Related research

A direct CO2 control system for ocean acidification experiments: testing effects on the coralline red algae Phymatolithon lusitanicum.

PeerJ

Physiological response of the cold-water coral Desmophyllum dianthus to thermal stress and ocean acidification.

PeerJ

Host anemone size as a determinant of social group size and structure in the orange clownfish (Amphiprion percula)

PeerJ

The physiological response of the deep-sea coral Solenosmilia variabilis to ocean acidification

PeerJ

Primary producers may ameliorate impacts of daytime CO2 addition in a coastal marine ecosystem

PeerJ

Anatomical changes in the inner ear of the bullfrog across metamorphic development

Erika E. Alexander et al., Proceedings of Meetings on Acoustics, 2014

Temperature-dependent growth mechanisms of CaF2 on Si(111)

C. R. Wang et al., Journal of Vacuum Science & Technology A: Vacuum, Surfaces, and Films, 2004

Sudden Hearing Loss Associated With Yoga Breathing Exercise Bruce M. Gardner, MD, Medscape

Evidence of hearing loss due to dynamite fishing in two species of odontocetes Aude F. Pacini et al., Proceedings of Meetings on Acoustics, 2017

Preparation and topography analysis of randomly textured glass substrates Eerke Bunte et al., Journal of Vacuum Science & Technology A: Vacuum, Surfaces, and Films, 2010

Powered by TREND MD

PeerJ Job Listings List & find academic jobs on PeerJ for free. Learn more >